

# Long-Term Genistein Consumption Modifies Gut Microbiota, Improving Glucose Metabolism, Metabolic Endotoxemia, and Cognitive Function in Mice Fed a High-Fat Diet

Patricia López, Mónica Sánchez, Claudia Perez-Cruz, Laura A. Velázquez-Villegas, Tauqeerunnisa Syeda, Miriam Aguilar-López, Ana K. Rocha-Viggiano, María del Carmen Silva-Lucero, Ivan Torre-Villalvazo, Lilia G. Noriega, Nimbe Torres, and Armando R. Tovar\*

**Scope:** The aim of this study is to assess whether the long-term addition of genistein to a high-fat diet can ameliorate the metabolic and the cognitive alterations and whether the changes can be associated with modifications to the gut microbiota.

**Methods and results:** C57/BL6 mice were fed either a control (C) diet, a high-fat (HF) diet, or a high-fat diet containing genistein (HFG) for 6 months. During the study, indirect calorimetry, IP glucose tolerance tests, and behavioral analyses were performed. At the end of the study, plasma, liver, brain, and fecal samples were collected. The results showed that mice fed the HFG diet gained less weight, had lower serum triglycerides, and an improvement in glucose tolerance than those fed an HF diet. Mice fed the HFG diet also modified the gut microbiota that was associated with lower circulating levels of lipopolysaccharide (LPS) and reduced expression of pro-inflammatory cytokines in the liver compared to those fed HF diet. The reduction in LPS by the consumption of genistein was accompanied by an improvement of the cognitive function.

**Conclusions:** Genistein is able to regulate the gut microbiota, reducing metabolic endotoxemia and decreasing the neuroinflammatory response despite the consumption of a HF diet.

## 1. Introduction

In recent years, the biological effects of dietary bioactive compounds, particularly polyphenols, have been actively investigated.<sup>[1]</sup> These molecules present in foods can explain in part the health benefits attributed to the consumption of functional foods.<sup>[2,3]</sup> Several studies in vitro and in experimental animals have demonstrated that polyphenols have biological effects, which, in many instances, positively produce health benefits that have been assessed in epidemiological and clinical studies in humans.<sup>[1]</sup> The biological mechanisms by which polyphenols can produce these effects are not fully understood, and they are actively investigated in order to use these compounds as part of the strategies aimed at slowing or preventing the comorbidities associated with several chronic degenerative diseases, particularly those associated with obesity.<sup>[4,5]</sup>

P. López, M. Sánchez, Dr. L. A. Velázquez-Villegas,<sup>[+]</sup>  
M. Aguilar-López,<sup>[++]</sup> A. K. Rocha-Viggiano, Dr. I. Torre-Villalvazo,  
Dr. L. G. Noriega, Dr. N. Torres, Dr. A. R. Tovar  
Departamento de Fisiología de la Nutrición  
Instituto Nacional de Ciencias Médicas y Nutrición Salvador Zubirán  
Av. Vasco de Quiroga No. 15, Belisario Domínguez Sección XVI, 14080  
Ciudad de México, México  
E-mail: tovar.ar@gmail.com

Dr. C. Perez-Cruz, T. Syeda, Dr. M. del Carmen Silva-Lucero<sup>[+++]</sup>  
Departamento de Farmacología  
Centro de Investigaciones y de Estudios Avanzados del Instituto  
Politécnico Nacional  
Av. Politécnico Nacional 2508, San Pedro Zacatenco, 07360  
Ciudad de México, México

<sup>[+]</sup>Present address: Laura A. Velázquez-Villegas: Laboratory of Metabolic Signalling, Ecole Polytechnique Fédérale de Lausanne, Switzerland

<sup>[++]</sup>Present address: Miriam Aguilar-Lopez: Department Food Science and Human Nutrition, University of Illinois Urbana-Champaign, USA

<sup>[+++]</sup>Present address: María del Carmen Silva-Lucero: Universidad Politécnica de Huatusco, Veracruz, México

DOI: 10.1002/mnfr.201800313

In recent years, several studies have investigated whether these effects are in part related to potential interactions between these molecules and gut microbiota.<sup>[6,7]</sup> It is known that dysbiosis of the gut microbiota can be related to the development of obesity, as has been demonstrated in mouse and human studies.<sup>[8–10]</sup> Furthermore, changes in the abundance of specific species of the gut microbiota are associated with specific metabolic changes.<sup>[11]</sup> Obesity and dysbiosis can trigger chronic low-grade inflammation.<sup>[12,13]</sup> Activation of the inflammatory state by the microbial imbalance is in part mediated by changes in the gut permeability that allows for an increase in the concentration of circulating lipopolysaccharide (LPS), which stimulates toll-like receptor 4 (TLR4), increasing the concentration of pro-inflammatory cytokines and leading to metabolic endotoxemia.<sup>[14]</sup> Furthermore, LPS is known as a potent neuroinflammatory agent that can cause neurodegenerative-like changes in the brain. Therefore, metabolic products of gut bacteria can influence brain function and integrity. A link between obesity-induced gut dysbiosis and brain neuroinflammation may be related to cognitive impairment. In fact, mid-life obesity is considered a risk factor for developing late-life dementia and even Alzheimer's disease.<sup>[15]</sup>

Several studies have demonstrated that consumption of soy protein in animal and human studies improved lipid and carbohydrate metabolism. In particular, soy protein can reduce total and LDL cholesterol levels, attenuate hepatic steatosis in rats or mice fed high-fat diets, and improve insulin sensitivity in obese animals.<sup>[16–18]</sup> There is evidence that a part of these beneficial health effects is associated with its content of the isoflavones genistein and daidzein.<sup>[19,20]</sup> There is evidence that genistein may be involved in the biological mechanism of action of soy protein on lipid and carbohydrate metabolism.<sup>[19,20]</sup> In mice fed a high-fat (HF) diet, short-term genistein supplementation can stimulate fatty acid oxidation in skeletal muscle by increasing the phosphorylation of the enzyme adenosine monophosphate-activated protein kinase (AMPK).<sup>[20]</sup> In addition, genistein supplementation modulates the microbiome of humanized mice increasing the latency of breast tumor and reducing tumor growth.<sup>[21]</sup> However, there are few studies assessing whether genistein may generate a change in the gut microbiota. Recently, it was shown that genistein intake modulates gut microbiota diversity that was associated with a decrease in the plasma levels of pro-inflammatory cytokines in nonobese diabetic mice compared to the vehicle-treated group.<sup>[22]</sup> However, it has not been demonstrated whether genistein can modulate the gut–brain interaction.

Therefore, the aim of the present work was to study the effects of the long-term supplementation of genistein in mice fed an HF diet on the gut microbiota, biochemical and metabolic variables, and cognitive conduct to assess whether potential changes in the gut microbiota due to the dietary bioactive compound genistein can modify the brain–gut interaction.

## 2. Experimental Section

### 2.1. Animal Care and Maintenance

Nine-week-old male C57BL6 mice weighing approximately 20 g were housed in cages, maintained with a 12 h light/dark cycle at

**Table 1.** Composition of the experimental diets.

Ingredient [%]	C	HF	HFG
Casein	20	24	24
Cornstarch	39.7	28	27.8
Dextrose	13.2	9.4	9.4
Sucrose	10	7.4	7.4
Soy oil	7	2.5	2.5
Cellulose	5	5	5
Mineral mixture AIN-93M	3.5	3.5	3.5
Vitamin mixture AIN-93VX	1	2	2
Choline citrate	0.25	0.25	0.25
Cystine	0.3	0.3	0.3
Lard		17.7	17.7
TBHQ	0.0013	0.0013	0.0013
Genistein			0.2

22 °C, and randomly assigned to one of the following experimental diets ( $n = 8$  per group): control diet (C), high-fat diet (HF), or high-fat diet with 0.2% genistein (HFG). The dose of genistein that mice consumed was approximately  $3 \text{ mg kg}^{-1} \text{ d}^{-1}$  body weight. Genistein was obtained from LC Laboratories (Woburn, MA). The mice had free access to their experimental diets and water for 6 months. The diets were administered in dry form, and the composition of each diet is described in **Table 1**. The mice were weighed twice weekly, and food consumption was determined every day. On the last day of the treatment, the mice were anaesthetized with sevoflurane (Pisa Farmaceutica, Guadalajara, JAL., México). Then, blood was collected by cardiac puncture with a heparinized syringe and centrifuged at  $1000 \times g$  for 10 min. Plasma was frozen and stored at  $-70 \text{ °C}$  until analysis. Liver, adipose tissue, and brain samples were obtained for total RNA and protein extraction and for histological and immunohistochemical analyses. Tissues were placed immediately into liquid nitrogen and stored at  $-70 \text{ °C}$  until further determination. For histological analysis, a portion of the tissue was fixed in 10% formalin at  $4 \text{ °C}$ . The protocol used in this study was approved by the Animal Committee of the National Institute of Medical Sciences and Nutrition, Mexico City and complies with the National Institutes of Health guide for the care and use of Laboratory animals (NIH Publications No. 8023, revised 1978).

### 2.2. Indirect Calorimetry

In the fifth month, indirect calorimetry analysis was conducted. The mice were housed individually in metabolic chambers and maintained at  $22 \text{ °C}$  under a 12 h/12 h light–dark cycle. Food was available from 19:00 to 7:00 h, and water was available ad libitum. All of the mice were acclimatized to the monitoring cages for 24 h prior to the beginning of an additional 48 h of continuous recordings of physiological parameters. The results are shown as the average of two 12 h/12 h light–dark cycles during the 48 h study. The mice were weighed prior to each trial. All metabolic measurements were obtained using an open-circuit indirect calorimetry system (Comprehensive Lab Animal Monitoring System,

Columbus Instruments, OH). The analysis was performed using CLAX software as supplied by the manufacturer. The respiratory exchange ratio (RER) was calculated as the  $VCO_2/VO_2$  ratio during the 24 h period.

### 2.3. Intraperitoneal Blood Glucose Tolerance Test

Additionally, in the fifth month, an intraperitoneal glucose tolerance test (IPGTT) was carried out. The mice were fasted for 6 h before the test. The IPGTT was performed by the administration of  $2 \text{ g kg}^{-1}$  intraperitoneally injected glucose. Blood samples were obtained from the tail with a test strip at different time intervals, and glucose was measured with a OneTouch Ultra glucometer (Accu-Chek Sensor, Roche Diagnostics). The area under the curve (AUC) was calculated using the GraphPad PRISM version 7.0D program.

### 2.4. Behavioral Analysis

Five days before finalizing all dietary interventions, the animals were submitted to the T-maze spontaneous alternation test to assess working memory as previously described (Deacon and Rawlins, 2006). Briefly, the T-maze was made of transparent acrylic and consisted of three arms (two objective arms:  $50 \times 20 \times 30 \text{ cm}$ ; one starting arm:  $60 \times 30 \times 10 \text{ cm}$ ; and a central division:  $30 \times 10 \text{ cm}$ ). This test involves two phases. The *sample phase* consists of placing the animal at the starting arm and allowing it to choose between one of the two objective arms. During this phase, a central division is placed between the two objective arms. Once the animal has chosen an arm, it is enclosed and kept in this place for 30 s by closing a guillotine door. Afterward, the animal is removed from the T-maze and placed back into its home cage for 2 min. Next, the *choice phase* is performed. The animal is placed again at the starting arm but without the central division and is allowed to choose an arm. If the animal chooses a different arm than that chosen during the sample phase, it is considered an alternation. A total of three repetitions of sample-choice phases were done per animal each day, on two consecutive days. The proportion of correct answers (alternation of entry to an arm) was calculated per experimental group.

### 2.5. Plasma Measurements

The levels of fasting plasma glucose, triglycerides, total cholesterol, LDL, and HDL cholesterol were determined by using the biochemical analyzer COBAS (Roche Diagnostics, Indianapolis, IN). Serum LPS was measured using a competitive inhibition enzyme immunoassay (Cloud-Clone Corp, Houston, TX).

### 2.6. Immunohistochemistry in the Brain

At the end of the study, the brains were removed immediately, and the left hemisphere was immersed in a 4% fixative solution of paraformaldehyde for 48 h. Horizontal brain sections ( $40$

$\mu\text{m}$ ) were obtained from the hippocampal formation according to the Mouse Brain Atlas<sup>[23]</sup> (Bregma  $-1.82$  to  $-2.06$ ). All sections were immediately immersed in a cryoprotectant solution for light microscopy (300 g sucrose [J.T. Baker]; 400 mL 0.1 M PB, and 300 mL ethylene glycol [Sigma] for 1 L) and stored at  $-20^\circ\text{C}$  until use. Slides were permeabilized with 0.2% Triton X-100 in PBS (0.2% PBS-Triton) for 20 min. The sections were washed in PBS and incubated in 0.3%  $\text{H}_2\text{O}_2$  (in PBS) for 10 min to inactivate endogenous peroxidase activity, followed by three washing steps (10 min each, in 0.2% PBS-Triton). The sections were incubated in 5% BSA (bovine serum albumin; Sigma) in PBS for 15 min to block nonspecific antibody binding. Subsequently, incubation with the primary antibody against glial fibrillary acid protein (GFAP; 1:500, Cell Signaling) diluted in 0.2% PBS-Triton was performed overnight at  $4^\circ\text{C}$ . Thereafter, the sections were incubated for 2 h with secondary horseradish peroxidase-conjugated antibodies (Jackson ImmunoResearch) in 0.2% PBS-Triton. Hydrogen peroxide (0.01%) and DAB (0.06%) in 0.2% PBS-Triton were used to develop the horseradish peroxidase enzymatic reaction. The enzymatic reaction was stopped with 0.2% PBS-Triton. Finally, the sections were mounted on glass slides, left to dry overnight, and cover slipped with Entellan mounting medium (Merck). For image acquisition, a Nikon Eclipse 80i light microscope equipped with a Nikon DS-Ri1 camera was used to acquire bright-field images under a  $10\times$  objective. For astrocyte quantification, at least three slides from each animal were imaged from the stratum radiatum CA1 hippocampal region. The number of cells per area analyzed was scored in each slice.

### 2.7. Immunofluorescence in Adipose Tissue

The subcutaneous adipose tissue was dissected from the inguinal area, immediately fixed with ice-cold 4% w/v paraformaldehyde in PBS, embedded in paraffin and cut at  $4 \mu\text{m}$ . The sections were incubated at  $60^\circ\text{C}$  for 20 min, deparaffinized by immersion in xylene, and rehydrated through graded ethanol solutions. The sections were washed with 1X PBS and blocked with 10% rabbit serum (Santa Cruz Biotechnology) for 30 min at room temperature. The sections were then incubated with rabbit anti-uncoupling protein 1 (UCP1) diluted 1:100 (Abcam) at room temperature for 1 h. After washing with 1X PBS, the sections were incubated with goat anti-rabbit FITC-conjugated secondary antibody diluted 1:500 (Santa Cruz Biotechnology) at room temperature for 1 h. The sections were washed again with 1X PBS, mounted with UltraCruz mounting medium (Santa Cruz Biotechnology) and viewed under a Leica DM750 microscope (Leica, Wetzlar, Germany).

### 2.8. Histological Analysis of Adipose Tissue

Paraffin-embedded subcutaneous adipose tissue sections were stained with hematoxylin and eosin and imaged at  $20\times$  magnification. Analysis of the adipocyte areas was performed using Adiposoft software following the authors' instructions.<sup>[24]</sup>

## 2.9. Quantitative Real-Time PCR

Total RNA from adipose tissue was extracted according to Chomczynski and Sacchi<sup>[25]</sup> using TRIzol reagent (Invitrogen). Total RNA was subjected to quantitative real-time polymerase chain reaction (qPCR) using SYBR Green and primer sets (Applied Biosystems).  $\beta$ -Actin was used as an invariant control. The relative amounts of all mRNAs were calculated with the comparative CT method.

## 2.10. Western Blot Analysis

For the analysis of brain proteins, the right hemispheres were rapidly removed, and the prefrontal cortex (PFC) was dissected in an ice-cold glass dish. The samples were then snap-frozen in liquid nitrogen and kept at  $-80^{\circ}\text{C}$  until analysis. For the analysis of brain and adipose tissue proteins, tissues were homogenized in lysis buffer (50 mM Tris, pH 7.4; 8.50% sucrose; 2 mM EDTA, pH 8.0; 10 mM  $\beta$ -ME; 500  $\mu\text{M}$  AEBSF; 8  $\mu\text{g mL}^{-1}$  aprotinin; 10  $\mu\text{g mL}^{-1}$  leupeptin; 4  $\mu\text{g mL}^{-1}$  pepstatin A; 5 mM benzamide; 20 mM  $\beta$ -glycerophosphate; 10 mM NaF and 1 mM  $\text{Na}_3\text{VO}_4$ ), and the protein concentration was determined by the Lowry method. Proteins were separated on 10–12% SDS polyacrylamide gels and electroblotted onto PVDF membranes. The membranes were incubated overnight at  $4^{\circ}\text{C}$  with primary antibody against postsynaptic density 95 protein (PSD95; 1:1000, Sigma Aldrich), GFAP (1:1000; Cell Signaling), ionized calcium binding adaptor molecule 1 (Iba1), toll-like receptor 4 (TLR4), and peroxisome proliferator-activated receptor gamma coactivator 1 alpha (PGC-1 $\alpha$ ). The membranes were washed with TBS-T (TBS +0.05% Tween 20) and then incubated with a horseradish peroxidase (POD)-linked anti-rabbit secondary antibody (1:5000, Jackson ImmunoResearch). Immunoreactive bands were visualized by enhanced chemiluminescence ECL for routine immunoblotting. Data were analyzed by densitometry using Image Lab software (Bio-Rad). Values were normalized with  $\beta$ -actin and expressed as the fold increase.

## 2.11. Gut Microbiota

One day before tissue harvesting, a sample of feces from mice in each group was collected. The sample was stored in RNAlater (Thermo Fisher) solution until analysis. Fecal samples from mice were immediately collected and frozen at  $-70^{\circ}\text{C}$ . DNA extraction was carried out using a QIAamp DNA Stool Mini Kit (Qiagen, USA), according to the manufacturer's instructions. Variable regions 3–4 of the 16S rRNA gene were amplified using specific forward (5' TCGTCGGCAGCGTCAGATGTGTATAAGACAGCCTACGGGNGGCWGCAG 3') and reverse primers (5' GTCTCGTGGGCTCGGAGATGTGTATAAAGAGACAGGACTAC HVGGGTATCTAATCC 3') containing the Illumina adapter overhang nucleotide sequences. Ampure XP beads were used to purify the 16S V3-V4 amplicons, and they were quantified on an Agilent 2100 Bioanalyzer (Agilent Technologies, USA). The amplicon size was approximately 550 bp. An index PCR was then carried out to attach dual indices using a Nextera XT

v2 Kit. The amplicon size was approximately 610 bp, and the concentration of double-stranded DNA was measured using a fluorometer Qubit 3.0 with a high-sensitivity kit. The final amplicon library was pooled in equimolar concentrations. Sequencing was performed on the Illumina MiSeq platform (MiSeq Reagent Kit V.3, 600 cycles) according to the manufacturer's instructions to generate paired-end reads of 300 bases in length in each direction.

## 2.12. Sequence Analysis

For taxonomic composition analysis, Custom C# and python scripts in the Quantitative Insights Into Microbial Ecology (QIIME) software pipeline 1.9 were used to process the sequencing files.<sup>[26]</sup> The sequence outputs were filtered for low-quality sequences (defined as any sequences that are  $<200$  bp or  $>620$  bp, sequences with any nucleotide mismatches to either the barcode or the primer, sequences with an average quality score of  $<25$ , and sequences with ambiguous bases  $>0$ ). Sequences were checked for chimeras with Gold.fai, and chimeric sequences were filtered out. The analysis started by clustering sequences within a percent sequence similarity into operational taxonomic units (OTUs). Ninety-one percent of the sequences passed filtering, resulting in 48 008 sequences per sample on average with a 97% similarity threshold. OTUs picking was performed with the tool set from QIIME, using the Usearch method.<sup>[27]</sup> OTUs were picked against the GreenGenes v.13.9 database. Ninety-seven percent of the OTUs were selected from the database. After the resulting OTU files were merged into one overall table, taxonomy was assigned based upon the GreenGenes reference taxonomy database. Thus, 99.79%, 97.18%, 97.07%, 82.92%, 58.52%, and 7.37% of the reads were assigned to the phylum, class, order, family, genus, and species level, respectively. Species richness (Observed, Chao1) and alpha diversity measurements (Shannon) were calculated, and we estimated the within-sample diversity at a rarefaction depth of  $>17\ 351$  reads per sample. Weighted and unweighted UniFrac distances were used to perform the principal coordinate analysis (PCoA).

Microbial sequence data were pooled for OTUs comparison and taxonomic abundance analysis but separated by batch in the principle coordinates analysis (PCoA) to have clear PCoA figures. For even sampling, a depth of 14 002 sequences per sample was used. PCoAs were produced using Emperor, and the community diversity was determined by the number of OTUs and beta diversity, measured by UniFrac unweighted and weighted distance matrices in QIIME. ANOSIM, a permutational multivariate analysis of variance, was used to determine statistically significant clustering of groups based upon microbiota structure distances.

## 2.13. Statistical Analysis

Data are expressed as means  $\pm$  SD. The differences between groups were analyzed with one-way ANOVA, followed by Tukey's or Bonferroni's post hoc test. Differences were considered statistically significant when the  $p$ -value was less than 0.05, significant

differences are indicated with letters, where  $a > b > c$ . Statistical analyses were performed with GraphPad Prism version 7.0.

### 3. Results

#### 3.1. Weight Gain and Food Intake

To evaluate the protective effect of genistein on the development of metabolic alterations in mice with diet-induced obesity, we fed mice with a high-fat diet for 6 months. First, we evaluated the effect of the different dietary treatments on weight gain. Mice fed a control diet gained 13.2 g by the end of the study, whereas those fed an HF diet gained an average of 23 g ( $p < 0.01$ ). Interestingly, mice fed an HF diet containing genistein gained significantly less weight (13%) than those consuming only an HF diet, particularly after day 150 of the study (Figure 1A,B). Despite the difference in weight gain among the three groups, there was no significant difference in food intake expressed as g per day or as kcal per day (Figure 1C,D). Nonetheless, mice fed an HF diet had significantly greater liver weights than the groups fed a control or an HFG diet, but there were no significant differences between these two groups (Figure 1E).

#### 3.2. Energy Expenditure and WAT Browning Markers

We then assessed whether the lower weight gain of the mice fed an HFG diet compared to those fed an HF diet was due to a change in energy expenditure. Our data showed that the consumption of an HFG diet increased  $VO_2$  consumption compared to the intake of an HF diet alone (Figure 1F,G). Interestingly, this increase in  $VO_2$  was accompanied by a significant decrease in the respiratory exchange ratio (RER) during the dark cycle in mice fed an HFG diet with respect to those fed an HF diet (Figure 1H,I). To explore potential mechanisms by which genistein can increase  $VO_2$ , we assessed the expression of browning markers in WAT. Interestingly, qPCR, western blot, and immunohistochemistry analyses revealed an increase in the expression of UCP1 in subcutaneous adipose tissue (Figure 2A–C), as well as TBX1 mRNA and protein abundance (Figure 2D,E) and PRDM16 gene expression (Figure 2F), both markers of WAT browning. The increase in browning markers was associated with reduced adipose tissue weight and adipocyte size (Figure 2G,H). These results indicate that genistein, by an unknown mechanism, can activate subcutaneous adipose tissue fat oxidation, leading to a reduction in fat accumulation.

#### 3.3. Serum Lipids and Glucose Tolerance Test

Next, we assessed whether the increase in energy expenditure and the reduction in adipose tissue mass could modify lipid and carbohydrate metabolism. Feeding mice with an HF diet for 6 months increased serum triglycerides and total and LDL cholesterol (Figure 3A–C). Interestingly, the addition of genistein to an HF diet significantly decreased serum triglycerides; however, despite the differences in total and LDL cholesterol

between the groups, these differences did not reach statistical significance. We then assessed whether the addition of genistein to an HF diet could modify the glucose response to an IPGTT. Although mice fed an HF or an HFG diet did not show a significant difference in fasting blood glucose levels (Figure 3D), the addition of genistein significantly attenuated the elevation of blood glucose during the test compared to mice fed an HF diet. Consequently, we observed a significant reduction in the area under the curve of IPGTT in mice fed an HFG diet versus those fed only an HF diet (Figure 3E,F). There is recent evidence that the abnormalities in the metabolic profile related to an HF diet are associated with changes in the gut microbiota.

#### 3.4. Gut Microbiota Analysis

Thus, we assessed whether the consumption of genistein had an effect on the gut microbiota. With the sequencing analysis of the 16S rRNA, we first performed an alpha diversity analysis. The number of OTUs, as well as the Shannon index, was higher in the HFG group compared to the HF group (Figure 4A), and these metrics showed a similar behavior using rarefaction curve analysis. According to the GreenGenes database, reads were assigned to five phyla, 33 families, and 41 genera. Bacteroidetes, Firmicutes, and Proteobacteria represented  $\approx 95\%$  of the total sequences at the phylum level. The rest of the sequences belonged to Verrucomicrobia, TM7, Deferribacteres, Tenericutes, Cyanobacteria, Spirochaetes, and Actinobacteria. At this taxonomic level, the inclusion of genistein into an HF diet decreased the relative abundance of Bacteroidetes from 67.1% to 56.8%, whereas Firmicutes increased from 21.3% in the HF group to 26.8% in the HFG group. Although Verrucomicrobia only represented 1.44% of the total sequences, there was a 1.56-fold increase in mice fed an HF diet with genistein (Figure 4B).

The bacterial family composition also presented shifts in response to the dietary treatment. The relative abundance of Bacteroidaceae was higher in the HF group than in the HFG group, at 46.1% and 28.0%, respectively. However, Prevotellaceae and Verrucomicrobia were the main families that were higher in the HFG group than in the HF group (1.38% vs 0.08% and 3.52% vs 0.35%, respectively). This pattern was consistent at the genus level, where the relative abundance of *Bacteroides* was smaller in the HFG group (42.75%) than in the HF group (61.8%) and the relative abundances of *Prevotella* and *Akkermansia* were higher in the HFG group (2.23% and 5.75%) than in the HF group (0.10% and 0.47%). On the other hand, we also observed an increase in the *Faecalibacterium* genus in the HFG group (0.30%) compared to that in the HF group ( $p < 0.0001\%$ ) (Figure 4C). A heatmap was created to determine the differences between groups at the species level. This heatmap showed that the changes in the genus *Bacteroides* were mainly due to the shift of *Bacteroides acidifaciens* and *Bacteroides uniformis* and that the relative abundances of these species were lower in the group that consumed genistein in the diet (HFG). However, the increase in the genus *Prevotella* was mainly due to *Prevotella copri* and to a lesser extent *Prevotella stercorea*. Finally, the increase in the genus *Akkermansia* was due to the species *Akkermansia muciniphila* (Figure 4D).

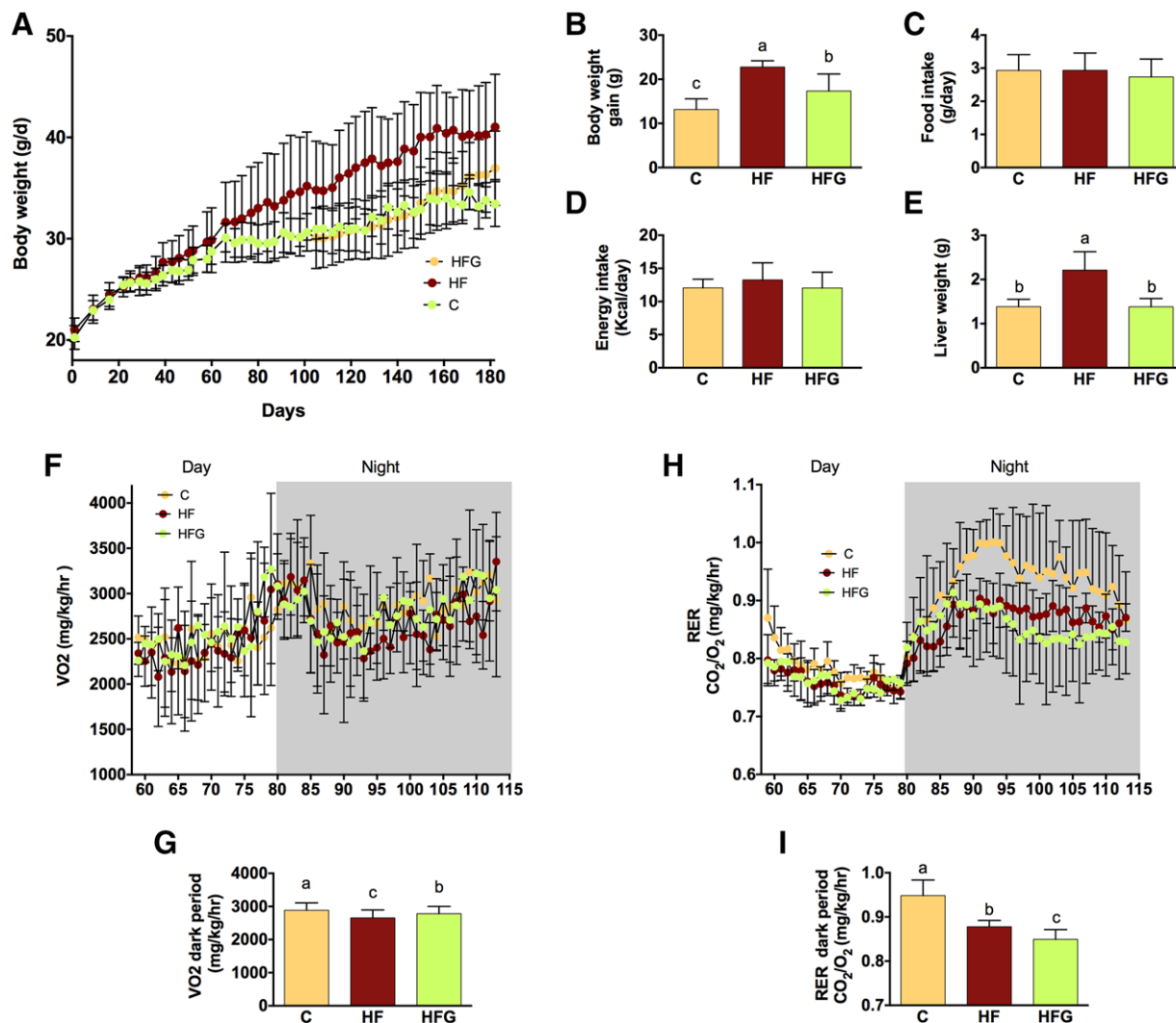


**Figure 1.** Genistein decreases body weight gain without altering food intake in mice fed a high-fat diet by increasing energy expenditure. Mice were fed a control diet (C), a high-fat diet (HF), or an HF diet supplemented with 0.2% genistein (HFG) for 6 months to evaluate A) weight gain during the experimental period, B) body weight gain by the end of the study, C) mean food intake during the experimental period expressed as grams per day, D) mean energy intake expressed as kcal per day, E) liver weight at the end of the study, F) oxygen consumption during two 12 h/12 h light–dark cycles, G) mean oxygen consumption during the feeding (night) period, H) respiratory exchange ratio (RER) during two 12 h/12 h light–dark cycles and I) mean RER during the feeding (night) period. Data are expressed as mean  $\pm$  SEM. The differences between groups were analyzed with one-way ANOVA, followed by Tukey's or Bonferroni's post hoc test. Differences were considered statistically significant when  $p < 0.05$ . Significant differences are indicated with letters, where  $a > b > c$ .

### 3.5. Lipopolysaccharide Circulating Levels

The dysbiosis produced in response to an HF diet is associated with an increase in circulating levels of LPS. An increase in circulating LPS has been demonstrated to trigger the inflammatory state in the body during obesity, leading to metabolic endotoxemia.<sup>[13]</sup> Our results clearly demonstrated that in mice fed an HF diet, LPS levels dramatically increased compared to those in C mice ( $p < 0.0001$ ). Surprisingly, the addition of genistein to a high-fat diet reduced LPS levels by 98.5% (Figure 5A). This result indicates that this polyphenol could reduce metabolic abnormalities in lipid and carbohydrate metabolism by ameliorating inflammation. Our results are in agreement with previous work that has demonstrated that an increase in *A. muciniphila*

improves the gut barrier by increasing the mucous layer, thus preventing the influx of LPS.<sup>[28]</sup>

### 3.6. Hepatic Expression of Protein Involved in the Inflammatory Response

To assess whether the increase in LPS in mice fed an HF diet increased the expression of proteins involved in the inflammatory response in the liver, we measured the expression of TLR4, TNF- $\alpha$ , IL-6, and IL-1 $\beta$  (Figure 5B–E). The results clearly showed that an HF diet induced a significant increase in the expression of TLR4, TNF- $\alpha$ , and IL-6 compared to that in the C group.

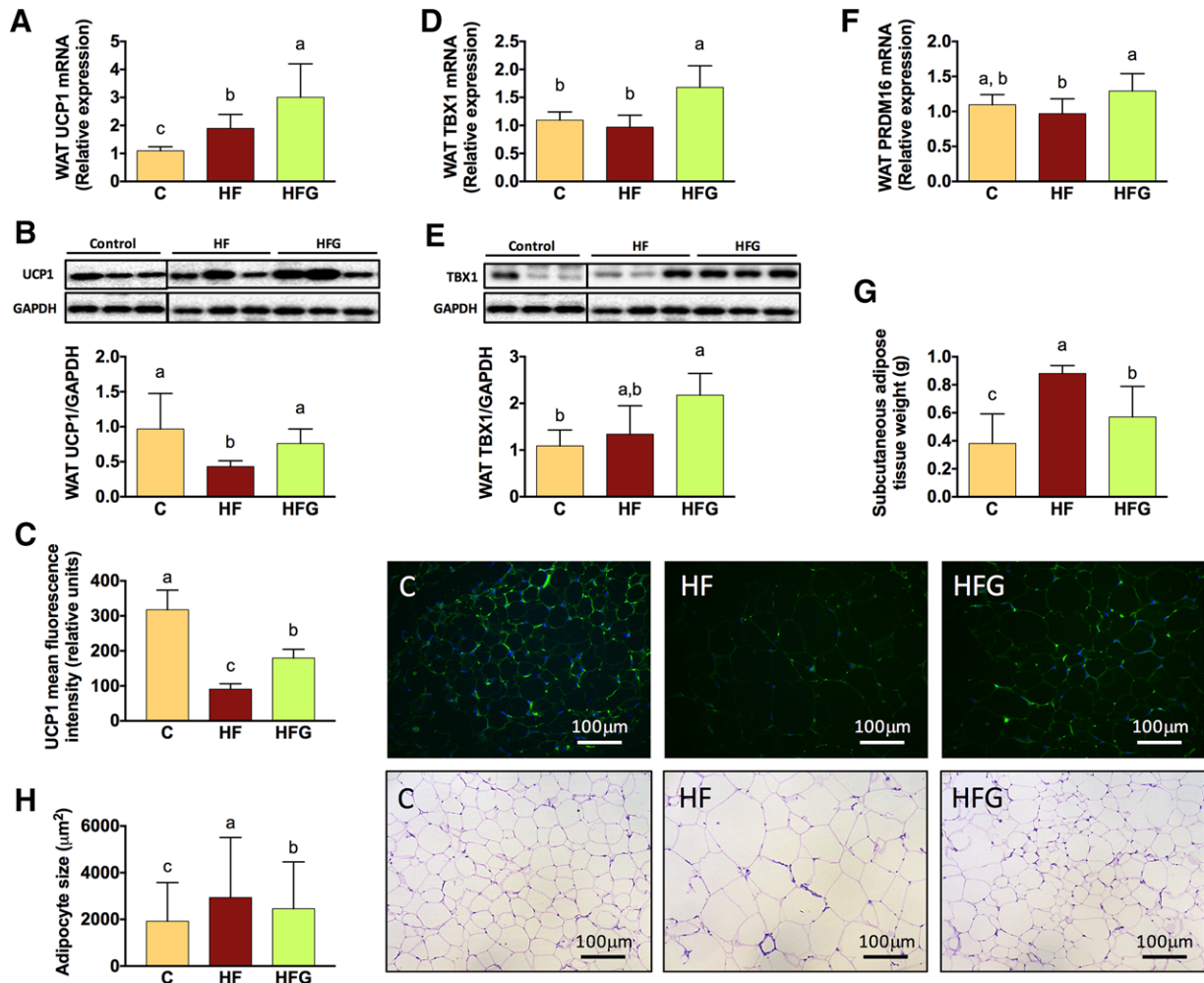


**Figure 2.** Genistein stimulates WAT browning in mice fed a high-fat diet. Mice were fed a control diet (C), a high-fat diet (HF), or an HF diet supplemented with 0.2% genistein (HFG) for 6 months to evaluate A) UCP1 mRNA abundance, B) UCP1 protein abundance, C) UCP1 immunofluorescence, D) TBX1 mRNA abundance, E) TBX1 protein abundance, F) PRDM16 mRNA abundance in subcutaneous white adipose tissue, G) subcutaneous adipose tissue weight at the end of the study, and H) mean adipocyte size. For western blots, each band represents an individual mice. Data are expressed as mean  $\pm$  SEM. The differences between groups were analyzed with one-way ANOVA, followed by Tukey's or Bonferroni's post hoc test. Differences were considered statistically significant when  $p < 0.05$ . Significant differences are indicated with letters, where  $a > b > c$ .

Interestingly, similar to LPS levels in the group fed an HFG diet, the three biomarkers of inflammation were significantly reduced to levels comparable to those observed in the control group.

### 3.7. Cognitive Analysis and Expression of Brain Proteins

The chronic inflammatory state observed in obese humans and rodents is associated with cognitive damage.<sup>[29,30]</sup> We then assessed whether genistein modulation of the gut microbiota and biochemical variables were associated with an improvement in cognitive abilities using the T-maze test. We observed that mice fed an HF diet had hippocampus-related memory impairments since a lower spontaneous alternation rate was observed in these mice than in C mice ( $p < 0.001$ ); However, genistein treatment improved memory rates in the HFG mice comparable to the levels of C group (HFG vs HF,  $p < 0.05$ ) (Figure 5F).

It has been widely described that cognitive abilities decline by the consumption of an HF diet, mainly affecting hippocampus and prefrontal cortex (PFC) functions.<sup>[31]</sup> Thus, we assessed the abundance of specific PFC proteins. We first studied the expression of postsynaptic proteins, particularly PSD-95. The relative amount of PSD-95 decreased in the HF mice compared to the C mice ( $p < 0.001$ ), while the HFG mice showed an increase in PSD-95 protein content in the brain cortex (HFG vs HF,  $p < 0.05$ ) (Figure 5G). As mitochondrial biogenesis improves synaptic function, we also evaluated the levels of PGC-1 $\alpha$  protein in the brain samples. There was a significant increase in PGC-1 $\alpha$  levels in the HFG mice compared to the C and the HF groups ( $p < 0.05$ ), and no difference was observed between these two groups (Figure 5H).

To evaluate the rate of neuroinflammation mediated by astrocyte and microglia cells in the hippocampus, we assessed the GFAP marker by immunohistochemical analysis. Reactive

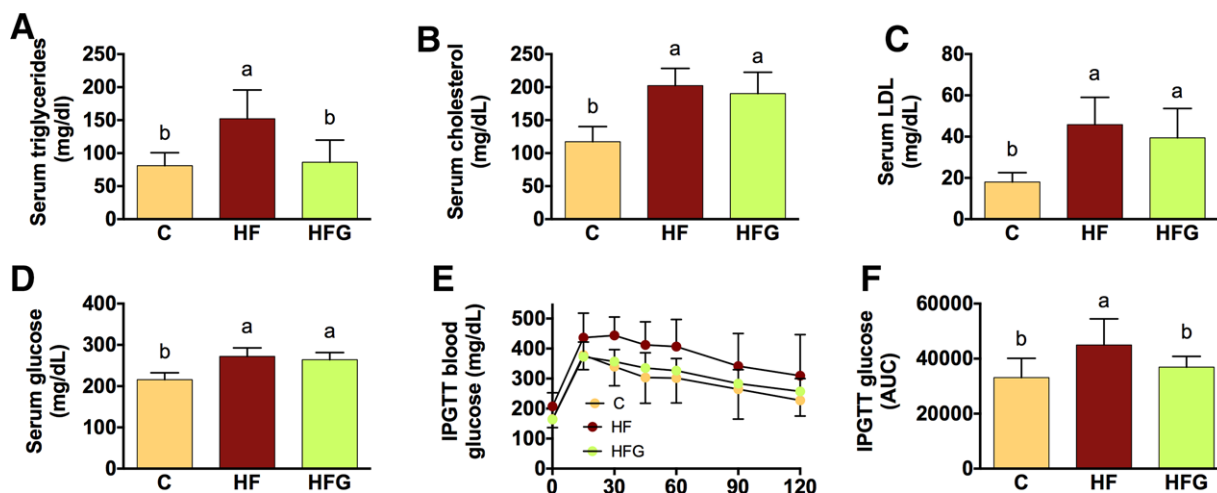


**Figure 3.** Genistein decreases serum lipids and improves glucose tolerance in mice fed a high-fat diet. Mice were fed a control diet (C), a high-fat diet (HF), or an HF diet supplemented with 0.2% genistein (HFG) for 6 months to evaluate A) serum triglycerides, B) total cholesterol, C) LDL cholesterol, D) serum glucose, E) glucose during the intraperitoneal glucose tolerance test (IPGTT), and F) the IPGTT area under the curve (AUC). Data are expressed as mean  $\pm$  SEM. The differences between groups were analyzed with one-way ANOVA, followed by Tukey's or Bonferroni's post hoc test. Differences were considered statistically significant when  $p < 0.05$ . Significant differences are indicated with letters, where  $a > b > c$ .

astrocytes were identified with GFAP. GFAP-positive cells increased in the hippocampus of the HF mice compared to those of the C mice ( $p < 0.0001$ ). The hippocampus of the HFG mice had a significant reduction in the number of GFAP-positive cells with respect to those of the HF mice (HF vs HFG,  $p < 0.0001$ ) (Figure 5I). Activation of microglia was detected by measuring Iba1 protein content in the PFC. Western blot analysis revealed that mice with an HF diet presented a significant increase in Iba1 compared to the C mice. Interestingly, the HFG mice presented a decrease in Iba1 levels compared to the HF group ( $p < 0.05$ ) (Figure 5J).

As we mentioned above, LPS can induce macrophage activation and TLR4 overexpression.<sup>[32]</sup> Since we observed an increase in LPS plasma levels in HF mice, we hypothesized that LPS may induce microglia activation by TLR4 overexpression. Therefore, we evaluated TLR4 protein level in PFC. TLR4 levels were increased in the HF mice compared to the C mice ( $p < 0.05$ ), but in the HFG mice, there was a significant decrease comparable to the levels of C group ( $p < 0.01$  vs HF mice) (Figure 5K).

#### 4. Discussion

The results of this study demonstrated that the addition of genistein to an HF diet significantly reduced body weight gain and that this reduction was accompanied by improvement of several biochemical variables, particularly serum triglycerides and serum insulin, leading to better glucose tolerance compared to an HF diet alone. In addition, these changes were accompanied by an increase in energy expenditure as well as an increase in WAT browning markers, indicating that genistein can stimulate thermogenesis. Nonetheless, mice fed HFG had a change in weight gain after day 150 of the study and this might be due to the phenotypic characterization of mice, which included glucose tolerance test and the calorimetry analysis. This evidence is in agreement with previous studies that have demonstrated that the isoflavone

genistein can improve metabolic variables, particularly those related to glucose metabolism.<sup>[20,33,34]</sup>

In addition, the present study demonstrated that genistein can in part regulate the changes in the metabolic profile by modifying the gut microbiota. Several studies have demonstrated that long-term consumption of a high-fat diet alters the gut microbiota.<sup>[8–10]</sup> The dysbiosis generated during obesity has been established as a key factor involved in the development of metabolic abnormalities.<sup>[35,36]</sup> The first studies indicated that during obesity, there was an alteration in the main phyla of the gut microbiota, especially in Firmicutes and Bacteroidetes.<sup>[37]</sup> However, recent evidence suggests that specific bacterial species in the gut microbiota are responsible for several of the biological effects. For instance, it has been demonstrated that *A. muciniphila* can improve insulin sensitivity and is associated with a decrease in the size of adipocytes.<sup>[11]</sup> Our study demonstrated that a single bioactive compound, such as genistein, is able to modulate the abundance of specific species of the gut microbiota. Specifically, our findings showed that genistein was able to increase the abundance among the *Prevotella* and *Akkermansia* genera, particularly *P. copri* and *A. muciniphila*. In fact, other bioactive compounds such as those found in *Agave salmiana* and pomegranate are reported to modulate the gut microbiota composition in mice<sup>[4]</sup> and humans,<sup>[38]</sup> reinforcing the potential therapeutic use of plant-derived bioactive compounds.

It has been found that the presence of certain specific species is associated with an increase in the expression of proteins that are involved in the formation of tight junctions in the intestinal epithelium, such as occluding.<sup>[5]</sup> Consequently, there is a decrease in the permeability of the intestinal lining, preventing the entrance of pro-inflammatory molecules into the body, particularly LPS. The mechanism by which LPS modifies gut permeability has been recently established. It has been demonstrated that LPS is able to reduce the expression of occludin and ZO-1 proteins, increasing paracellular permeability and epithelial barrier damage.<sup>[39]</sup> On the other hand, it has been recently described



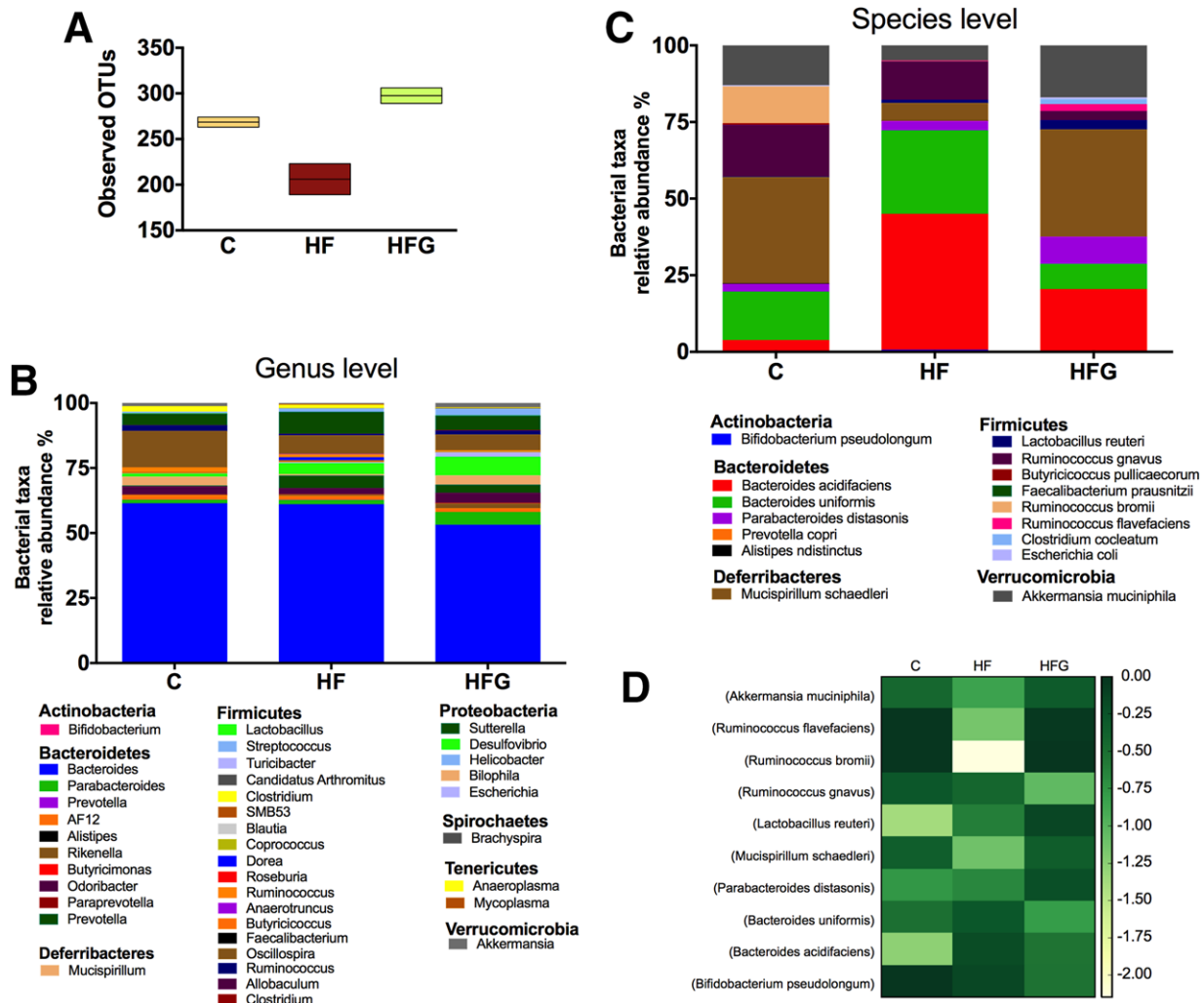


**Figure 4.** Genistein increases the diversity of the gut microbiota and specifically increases *Prevotella copri* and *Akkermansia muciniphila*. Mice were fed a control diet (C), a high-fat diet (HF), or an HF diet supplemented with 0.2% genistein (HFG) for 6 months to evaluate A) an alpha diversity analysis by clustering sequences within a percent sequence similarity into operational taxonomic units (OTUs), bacterial taxonomy at the B) genus and C) species levels, and D) the heatmap indicating differences at the level. A permutational multivariate analysis of variance (ANOSIM) was used to determine statistically significant clustering of groups based upon microbiota structure distances.

that LPS can activate the membrane-associated protein focal adhesion kinase and MyD88, leading to an increase in intestinal tight junction permeability.<sup>[40]</sup> As a consequence, there is an increase in paracellular transport, resulting in leaky gut, and additionally, there is an increase in transcellular LPS transport via chylomicrons, leading to elevated levels of circulating LPS<sup>[41]</sup> generating metabolic endotoxemia.<sup>[12]</sup> In this study, there was a dramatic decrease in the circulating levels of LPS in the mice fed genistein, despite the high-fat content in the diet, compared to mice consuming just the HF diet. The decrease in LPS in the mice fed an HF diet containing genistein was associated with significant improvement in metabolic variables, especially glucose tolerance, and with a decrease in the expression of inflammatory cytokines.

On the other hand, in addition to the negative systemic effects of obesity on metabolic parameters, recent studies have documented that brain cognitive functions are altered in

obese animal models. Obesity causes memory and learning difficulties<sup>[29,42,43]</sup> associated with an increase in neuroinflammation and amyloidosis.<sup>[5,44]</sup> Interestingly, in adipose tissue from obese subjects<sup>[44]</sup> and obese animal models,<sup>[45]</sup> there is an increase in amyloid precursor protein (APP), a protein associated with Alzheimer's pathology. Recently, obesity has been linked to the development of late-life dementia and represents a risk factor for Alzheimer's disease.<sup>[15]</sup>

In this study, we observed impairment in short-term memory in the HF mice, while genistein treatment improved cognition. Importantly, this improvement was accompanied by an increase in PSD95 protein in the brain cortex. A decrease in PSD95 protein in the brain correlates with cognitive impairment.<sup>[46]</sup> PSD95 is a protein associated with synaptic plasticity and is anchored at the postsynaptic sites of neurons, called dendritic spines.<sup>[47]</sup> Previous work has shown that genistein was able to rescue spatial learning and restore spine number in the cerebral cortex of

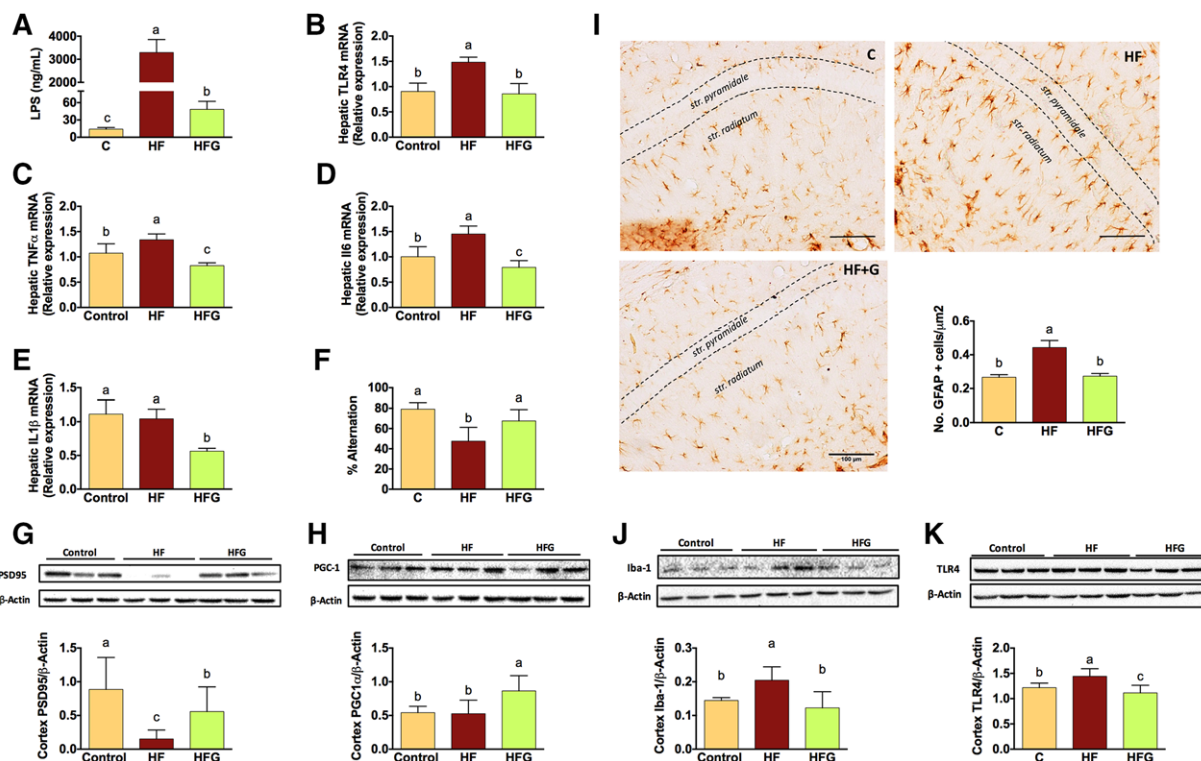


**Figure 5.** Genistein decreases circulating lipopolysaccharide and hepatic expression of inflammatory markers, improves cognitive behavior and decreases the expression of proteins involved in neuroinflammation in mice fed a high-fat diet. Mice were fed a control diet (C), a high-fat diet (HF), or an HF diet supplemented with 0.2% genistein (HFG) for 6 months to evaluate A) circulating lipopolysaccharide (LPS) content, hepatic mRNA abundance of B) TLR4, C) TNF- $\alpha$ , D) IL-6, and E) IL1 $\beta$ . F) Memory and spatial learning were assayed in a T-maze spontaneous alternation test; G) PSD95 and H) PGC-1 $\alpha$  protein abundance in the brain cortex. For western blots, each band represents an individual mice. I) GFAP immunohistochemistry in the hippocampus and J) Iba-1 and K) TLR4 protein abundance in the brain cortex. Data are expressed as mean  $\pm$  SEM. The differences between groups were analyzed with one-way ANOVA, followed by Tukey's or Bonferroni's post hoc test. Differences were considered statistically significant when  $p < 0.05$ . Significant differences are indicated with letters, where  $a > b > c$ .

surgically oestropausal young females.<sup>[48]</sup> Thus, genistein cognitive effects in the HF+G mice might be associated with an increased number of functional dendritic spines. In this respect, mitochondrial biogenesis is directly associated with improved synaptic function.<sup>[49]</sup> Specifically, peroxisome proliferator-activated receptor c co-activator 1a (PGC-1 $\alpha$ ) expression is associated with the formation and maintenance of neuronal dendritic spines.<sup>[49]</sup> Our data showed that genistein increased PGC-1 $\alpha$  content in the brain cortex, an event that might be associated with improved synaptic function (PSD95) and cognitive performance in the HFG mice.

Obesity can also induce macrophage proliferation and increase overexpression of TLR4 and other pattern recognition receptors.<sup>[50]</sup> In the brain, two types of cells mediate inflammatory reactions: microglia, which are the primary mediators of the central nervous system immune defense system,<sup>[51]</sup> and astrocytes,<sup>[52]</sup> activated microglia produce pro-inflammatory mediators that can be neurotoxic to cells.<sup>[53]</sup> Glial cells reactively respond to microbial infections by recognizing conserved motifs expressed by pathogens,<sup>[54]</sup> such as LPS.<sup>[55]</sup> In this study, we observed an increased number of GFAP-positive cells in the hippocampus and a nonsignificant increase in iba1 protein in the cortex of the HF mice. Since we observed an increase in LPS plasma levels in the HF mice, we assessed TLR4 protein content

in the brain samples. As expected, the HF mice showed higher TLR4 content in the brain cortex, but genistein ingestion reduced those levels lower than even those of the C mice. This finding may suggest that LPS and related pro-inflammatory cytokines associated with the HF-microbiota composition activate glia cells in the brain. This activation may impair the protective role of glia cells to maintain synaptic integrity and function, resulting in a decreased level of PSD95 protein and causing cognitive impairment. In this regard, it has been demonstrated that genistein is able to abate the LPS-induced inflammatory response through AMPK activation in macrophages.<sup>[56]</sup>

Genistein supplementation has been used in long-term clinical trials spanning from 2 to 4 years at doses from 50 to 200 mg per day.<sup>[57–62]</sup> It is important to emphasize that none of these studies reported any adverse effects in breast structure, bone mineral content, or circulating thyroid profile. Although the human equivalent dose of genistein that mice received in the present study according to Reagan-Show<sup>[63]</sup> was approximately 1.5 g per day for a 65 kg adult person, the evidence in other studies demonstrate that there are other factors that influence the absorption and bioavailability of genistein. It has been reported in mice that consumption of a diet containing 0.15% genistein, raised serum genistein levels to 3.81  $\mu$ mol L<sup>-1</sup>.<sup>[64]</sup> Interestingly, it has been reported in Japanese population that consumption of six to seven

servings of soy per week raises genistein concentration in serum to approximately  $1.5 \mu\text{mol L}^{-1}$ . Thus, these results suggest that humans have higher absorption of dietary genistein than mice,<sup>[65]</sup> requiring a lower dose to reach similar serum concentration of genistein. In addition, the chemical form of genistein, as aglycone or glucoside, can affect its intestinal absorption and plasma concentration, where the aglycone has higher bioavailability than the glucoside.<sup>[66]</sup> Nonetheless, dose-effect studies are necessary to establish the therapeutic window of the genistein biological effects to determine the minimum effective dose of genistein in order to translate this study to humans.

## 5. Conclusions

Our study demonstrated that genistein, a dietary bioactive compound that is present mainly in soy protein, can improve glucose metabolism in mice fed a high-fat diet. These benefits were accompanied by an increase in the proportion of two specific species of gut microbiota, *P. copri* and *A. muciniphila*. In addition, the results suggest that the increase in the *Prevotella* and *Akkermansia* genera was associated with a reduction in circulating levels of LPS. Therefore, the reduction in this pro-inflammatory molecule has a beneficial effect in the brain by decreasing neuroinflammation, suggesting that a single bioactive compound can modify the gut-brain interaction. It is important to point out that the present results obtained in a rodent model of obesity must be validated in a clinical trial in order to determine the effect of genistein in the brain-gut axis of obese humans. Therefore, a call for caution should be made to avoid extrapolating results and conclusions from research on animal models to humans; moreover, basic research in animal models should be viewed as the first step in the discovery pathway. In this regard, the present results open a new window for the use of specific dietary bioactive compounds as agents that can improve the metabolic and cognitive statuses that are altered during obesity.

## Acknowledgements

This work was funded by CONACYT (ART 261843). A.R.T. and N.T. did conception and design; P.L. and A.K.R.-V. conducted the research; P.L. and L.A.V.-V. performed western blot analysis; L.G.N. and P.L. did blood glucose tolerance curve and calorimetry analysis; I.T.-V. conducted histology and immunohistochemistry analyses; M.A.-L. and M.S. performed microbiota analysis; C.P.-C., T.S., and M.C.S.-L. performed brain analysis; A.R.T., N.T., L.A.V.-V., and M.A.-L. did data management; A.R.T., N.T., P.L., L.A.V.-V., and M.A.-L. performed statistical analyses, interpretation, drafting of the manuscript. A.R.T. had primary responsibility for the final content.

## Conflict of Interest

The authors declare no conflict of interest.

## Keywords

cognitive damage, genistein, gut microbiota, lipopolysaccharide, neuroinflammation

Received: March 31, 2018  
Revised: June 18, 2018  
Published online: July 30, 2018

- [1] S. G. J. van Breda, T. de Kok, *Mol. Nutr. Food Res.* **2018**, *62*, <https://doi.org/10.1002/mnfr.201700597>.
- [2] R. H. Liu, *Adv. Nutr.* **2013**, *4*, 384S.
- [3] A. Rodriguez-Casado, *Crit. Rev. Food Sci. Nutr.* **2016**, *56*, 1097.
- [4] A. M. Leal-Diaz, L. G. Noriega, I. Torre-Villalvazo, N. Torres, G. Aleman-Escondrillas, P. Lopez-Romero, M. Sanchez-Tapia, M. Aguilar-Lopez, J. Furuzawa-Carballeda, L. A. Velazquez-Villegas, A. Avila-Nava, G. Ordaz, J. A. Gutierrez-Urbe, S. O. Serna-Saldivar, A. R. Tovar, *Sci. Rep.* **2016**, *6*, 34242.
- [5] M. Sanchez-Tapia, M. Aguilar-Lopez, C. Perez-Cruz, E. Pichardo-Ontiveros, M. Wang, S. M. Donovan, A. R. Tovar, N. Torres, *Sci. Rep.* **2017**, *7*, 4716.
- [6] J. C. Espin, A. Gonzalez-Sarrias, F. A. Tomas-Barberan, *Biochem. Pharmacol.* **2017**, *139*, 82.
- [7] D. V. Seidel, M. A. Azcarate-Peril, R. S. Chapkin, N. D. Turner, *Semin. Cancer Biol.* **2017**, *46*, 191.
- [8] H. Plovier, P. D. Cani, *Microbiol. Spectr.* **2017**, *5*, <https://doi.org/10.1128/microbiolspec.BAD-0002-2016>.
- [9] P. J. Turnbaugh, *Cell Host Microbe.* **2017**, *21*, 278.
- [10] P. J. Turnbaugh, F. Backhed, L. Fulton, J. I. Gordon, *Cell Host Microbe.* **2008**, *3*, 213.
- [11] M. C. Dao, A. Everard, J. Aron-Wisniewsky, N. Sokolovska, E. Prifti, E. O. Verger, B. D. Kayser, F. Levenez, J. Chilloux, L. Hoyles, MICRO-Obes Consortium, M. E. Dumas, S. W. Rizkalla, J. Dore, P. D. Cani, K. Clement, *Gut* **2016**, *65*, 426.
- [12] P. D. Cani, J. Amar, M. A. Iglesias, M. Poggi, C. Knauf, D. Bastelica, A. M. Neyrinck, F. Fava, K. M. Tuohy, C. Chabo, A. Waget, E. Delmee, B. Cousin, T. Sulpice, B. Chamontin, J. Ferrieres, J. F. Tanti, G. R. Gibson, L. Casteilla, N. M. Delzenne, M. C. Alessi, R. Burcelin, *Diabetes* **2007**, *56*, 1761.
- [13] P. D. Cani, R. Bibiloni, C. Knauf, A. Waget, A. M. Neyrinck, N. M. Delzenne, R. Burcelin, *Diabetes* **2008**, *57*, 1470.
- [14] A. L. Neves, J. Coelho, L. Couto, A. Leite-Moreira, R. Roncon-Albuquerque, Jr., *J. Mol. Endocrinol.* **2013**, *51*, R51.
- [15] G. Livingston, A. Sommerlad, V. Orgeta, S. G. Costafreda, J. Huntley, D. Ames, C. Ballard, S. Banerjee, A. Burns, J. Cohen-Mansfield, C. Cooper, N. Fox, L. N. Gitlin, R. Howard, H. C. Kales, E. B. Larson, K. Ritchie, K. Rockwood, E. L. Sampson, Q. Samus, L. S. Schneider, G. Selbaek, L. Teri, N. Mukadam, *Lancet* **2017**, *390*, 2673.
- [16] C. Ascencio, N. Torres, F. Isoard-Acosta, F. J. Gomez-Perez, R. Hernandez-Pando, A. R. Tovar, *J. Nutr.* **2004**, *134*, 522.
- [17] L. Noriega-Lopez, A. R. Tovar, M. Gonzalez-Granillo, R. Hernandez-Pando, B. Escalante, P. Santillan-Doherty, N. Torres, *J. Biol. Chem.* **2007**, *282*, 20657.
- [18] A. R. Tovar, I. Torre-Villalvazo, M. Ochoa, A. L. Elias, V. Ortiz, C. A. Aguilar-Salinas, N. Torres, *J. Lipid Res.* **2005**, *46*, 1823.
- [19] M. Gonzalez-Granillo, K. R. Steffensen, O. Granados, N. Torres, M. Korach-Andre, V. Ortiz, C. Aguilar-Salinas, T. Jakobsson, A. Diaz-Villasenor, A. Loza-Valdes, R. Hernandez-Pando, J. A. Gustafsson, A. R. Tovar, *Diabetologia* **2012**, *55*, 2469.
- [20] B. Palacios-Gonzalez, A. Zarain-Herzberg, I. Flores-Galicia, L. G. Noriega, G. Aleman-Escondrillas, T. Zarinan, A. Ulloa-Aguirre, N. Torres, A. R. Tovar, *Biochim. Biophys. Acta* **2014**, *1841*, 132.
- [21] B. Paul, K. J. Royston, Y. Li, M. L. Stoll, C. F. Skibola, L. S. Wilson, S. Barnes, C. D. Morrow, T. O. Tollefsbol, *PLoS One* **2017**, *12*, e0189756.
- [22] G. Huang, J. Xu, D. E. Lefever, T. C. Glenn, T. Nagy, T. L. Guo, *Toxicol. Appl. Pharmacol.* **2017**, *332*, 138.
- [23] G. Paxinos, K. Franklin, *Paxinos and Franklin's the Mouse Brain in Stereotaxic Coordinates*, Academic Press, New York **2012**.

- [24] M. Galarraga, J. Campion, A. Munoz-Barrutia, N. Boque, H. Moreno, J. A. Martinez, F. Milagro, C. Ortiz-de-Solorzano, *J. Lipid Res.* **2012**, *53*, 2791.
- [25] P. Chomczynski, N. Sacchi, *Anal. Biochem.* **1987**, *162*, 156.
- [26] J. G. Caporaso, J. Kuczynski, J. Stombaugh, K. Bittinger, F. D. Bushman, E. K. Costello, N. Fierer, A. G. Pena, J. K. Goodrich, J. I. Gordon, G. A. Huttley, S. T. Kelley, D. Knights, J. E. Koenig, R. E. Ley, C. A. Lozupone, D. McDonald, B. D. Muegge, M. Pirrung, J. Reeder, J. R. Sevinsky, P. J. Turnbaugh, W. A. Walters, J. Widmann, T. Yatsunenko, J. Zaneveld, R. Knight, *Nat. Methods* **2010**, *7*, 335.
- [27] R. C. Edgar, *Bioinformatics* **2010**, *26*, 2460.
- [28] A. Everard, C. Belzer, L. Geurts, J. P. Ouwerkerk, C. Druart, L. B. Bindels, Y. Guiot, M. Derrien, G. G. Muccioli, N. M. Delzenne, W. M. de Vos, P. D. Cani, *Proc. Natl. Acad. Sci. U.S.A.* **2013**, *110*, 9066.
- [29] S. E. Kanoski, T. L. Davidson, *Physiol. Behav.* **2011**, *103*, 59.
- [30] A. A. Miller, S. J. Spencer, *Brain Behav. Immun.* **2014**, *42*, 10.
- [31] S. E. Kanoski, R. L. Meisel, A. J. Mullins, T. L. Davidson, *Behav. Brain Res.* **2007**, *182*, 57.
- [32] T. T. Wu, T. L. Chen, R. M. Chen, *Toxicol. Lett.* **2009**, *191*, 195.
- [33] S. Amanat, M. H. Eftekhari, M. Fararouei, K. Bagheri Lankarani, S. J. Massoumi, *Clin. Nutr.* **2018**, *37*, 1210.
- [34] K. Fang, H. Dong, D. Wang, J. Gong, W. Huang, F. Lu, *Mol. Nutr. Food Res.* **2016**, *60*, 1602.
- [35] K. Lippert, L. Kedenko, L. Antonielli, I. Kedenko, C. Gemeier, M. Leitner, A. Kautzky-Willer, B. Paulweber, E. Hackl, *Benef. Microbes.* **2017**, *8*, 545.
- [36] P. J. Parekh, L. A. Balart, D. A. Johnson, *Clin. Transl. Gastroenterol.* **2015**, *6*, e91.
- [37] R. E. Ley, P. J. Turnbaugh, S. Klein, J. I. Gordon, *Nature* **2006**, *444*, 1022.
- [38] A. Gonzalez-Sarrias, M. Romo-Vaquero, R. Garcia-Villalba, A. Cortes-Martin, M. V. Selma, J. C. Espin, *Mol. Nutr. Food Res.* **2018**, *62*, e1800160.
- [39] A. Bein, A. Zilbershtein, M. Golosovsky, D. Davidov, B. Schwartz, *J. Cell Physiol.* **2017**, *232*, 381.
- [40] S. Guo, M. Nighot, R. Al-Sadi, T. Alhmod, P. Nighot, T. Y. Ma, *J. Immunol.* **2015**, *195*, 4999.
- [41] K. Harris, A. Kassis, G. Major, C. J. Chou, *J. Obes.* **2012**, *2012*, 879151.
- [42] Z. A. Corder, K. L. Tamashiro, *Physiol. Behav.* **2015**, *152*, 363.
- [43] F. D. Heyward, D. Gilliam, M. A. Coleman, C. F. Gavin, J. Wang, G. Kaas, R. Trieu, J. Lewis, J. Moulden, J. D. Sweatt, *J. Neurosci.* **2016**, *36*, 1324.
- [44] Y. H. Lee, J. M. Martin, R. L. Maple, W. G. Tharp, R. E. Pratley, *Neuroendocrinology* **2009**, *90*, 383.
- [45] K. L. Puig, A. M. Floden, R. Adhikari, M. Y. Golovko, C. K. Combs, *PLoS One* **2012**, *7*, e30378.
- [46] R. Sultana, W. A. Banks, D. A. Butterfield, *J. Neurosci. Res.* **2010**, *88*, 469.
- [47] M. Migaud, P. Charlesworth, M. Dempster, L. C. Webster, A. M. Watabe, M. Makhinson, Y. He, M. F. Ramsay, R. G. Morris, J. H. Morrison, T. J. O'Dell, S. G. Grant, *Nature* **1998**, *396*, 433.
- [48] T. J. Wang, J. R. Chen, W. J. Wang, Y. J. Wang, G. F. Tseng, *PLoS One* **2014**, *9*, e89819.
- [49] A. Cheng, R. Wan, J. L. Yang, N. Kamimura, T. G. Son, X. Ouyang, Y. Luo, E. Okun, M. P. Mattson, *Nat. Commun.* **2012**, *3*, 1250.
- [50] M. Okla, W. Wang, S. Chung, *FASEB J.* **2016**, *30*, 291.2.
- [51] R. M. Ransohoff, V. H. Perry, *Annu. Rev. Immunol.* **2009**, *27*, 119.
- [52] S. A. Liddel, B. A. Barres, *Immunity* **2017**, *46*, 957.
- [53] V. H. Perry, C. Holmes, *Nat. Rev. Neurol.* **2014**, *10*, 217.
- [54] R. M. Ransohoff, M. A. Brown, *J. Clin. Invest.* **2012**, *122*, 1164.
- [55] I. C. Hoogland, C. Houbolt, D. J. van Westerloo, W. A. van Gool, D. van de Beek, *J. Neuroinflammation* **2015**, *12*, 114.
- [56] G. Ji, Y. Zhang, Q. Yang, S. Cheng, J. Hao, X. Zhao, Z. Jiang, *PLoS One* **2012**, *7*, e53101.
- [57] D. L. Alekel, U. Genschel, K. J. Koehler, H. Hofmann, M. D. Van Loan, B. S. Beer, L. N. Hanson, C. T. Peterson, M. S. Kurzer, *Menopause* **2015**, *22*, 185.
- [58] A. Bitto, F. Polito, M. Atteritano, D. Altavilla, S. Mazzaferro, H. Marini, E. B. Adamo, R. D'Anna, R. Granese, F. Corrado, S. Russo, L. Minutoli, F. Squadrito, *J. Clin. Endocrinol. Metab.* **2010**, *95*, 3067.
- [59] H. Fritz, D. Seely, G. Flower, B. Skidmore, R. Fernandes, S. Vadeboncoeur, D. Kennedy, K. Cooley, R. Wong, S. Sagar, E. Sabri, D. Ferguson, *PLoS One* **2013**, *8*, e81968.
- [60] H. Marini, A. Bitto, D. Altavilla, B. P. Burnett, F. Polito, V. Di Stefano, L. Minutoli, M. Atteritano, R. M. Levy, R. D'Anna, N. Frisina, S. Mazzaferro, F. Cancellieri, M. L. Cannata, F. Corrado, A. Frisina, V. Adamo, C. Lubrano, C. Sansotta, R. Marini, E. B. Adamo, F. Squadrito, *J. Clin. Endocrinol. Metab.* **2008**, *93*, 4787.
- [61] F. M. Steinberg, M. J. Murray, R. D. Lewis, M. A. Cramer, P. Amato, R. L. Young, S. Barnes, K. L. Konzelmann, J. G. Fischer, K. J. Ellis, R. J. Shypailo, J. K. Fraley, E. O. Smith, W. W. Wong, *Am. J. Clin. Nutr.* **2011**, *93*, 356.
- [62] A. H. Wu, D. Spicer, A. Garcia, C. C. Tseng, L. Hovanessian-Larsen, P. Sheth, S. E. Martin, D. Hawes, C. Russell, H. MacDonald, D. Tripathy, M. Y. Su, G. Ursin, M. C. Pike, *Cancer Prev. Res.* **2015**, *8*, 942.
- [63] S. Reagan-Shaw, M. Nihal, N. Ahmad, *FASEB J.* **2008**, *22*, 659.
- [64] A. Naaz, S. Yellayi, M. A. Zakroczymski, D. Bunick, D. R. Doerge, D. B. Lubahn, W. G. Helferich, P. S. Cooke, *Endocrinology* **2003**, *144*, 3315.
- [65] P. Fanti, T. J. Stephenson, I. M. Kaariainen, B. Rezkalla, Y. Tsukamoto, T. Morishita, M. Nomura, C. Kitiyakara, L. J. Custer, A. A. Franke, *Nephrol. Dial Transplant.* **2003**, *18*, 1862.
- [66] T. Izumi, M. K. Piskula, S. Osawa, A. Obata, K. Tobe, M. Saito, S. Kataoka, Y. Kubota, M. Kikuchi, *J. Nutr.* **2000**, *130*, 1695.